arXiv:1410.6490v1 [astro-ph.SR] 23 Oct 2014

Herschel observations of dust around the high-mass X-ray binary GX 301–2

M. Servillat[1,2,3], A. Coleiro[4,2], S. Chaty[2,5], F. Rahoui[6,3] and J. A. Zurita Heras[4]

ABSTRACT

We aim at characterising the structure of the gas and dust around the high mass X-ray binary GX 301–2, a highly obscured X-ray binary hosting a hypergiant star and a neutron star, in order to better constrain its evolution. We used *Herschel* PACS to observe GX 301–2 in the far infrared and completed the spectral energy distribution of the source using published data or catalogs, from the optical to the radio range (0.4 to 4×10^4 μm). GX 301–2 is detected for the first time at 70 and 100 μm. We fitted different models of circumstellar environments to the data. All tested models are statistically acceptable, and consistent with a hypergiant star at ∼3 kpc. We found that the addition of a free-free emission component from the strong stellar wind is required and could dominate the far infrared flux. Through comparisons with similar systems and discussion on the estimated model parameters, we favour a disk-like circumstellar environment of ∼8 AU that would enshroud the binary system. The temperature goes down to ∼200 K at the edge of the disk, allowing for dust formation. This disk is probably a rimmed viscous disk with an inner rim at the temperature of the dust sublimation temperature (∼1 500 K). The similarities between the hypergiant GX 301–2, B[e] supergiants and the highly obscured X-ray binaries (in particular IGR J16318–4848) are strengthened. GX 301–2 might represent a transition stage in the evolution of massive stars in binary systems, connecting supergiant B[e] systems to luminous blue variables.

Subject headings: X-rays: binaries, individuals: GX 301-2; Stars: early-type, evolution, circumstellar matter, individuals: BP Cru, Wray 977

1. Introduction

Massive stars (more than about eight times the mass of the Sun, e.g. Heger et al. 2003) have been key players in the cosmic history through their enormous input of ionizing photons, energy, momentum, and chemical species into the Universe. In addition, the hot, massive stars can episodically form enormous quantities of dust. The presence of dust and its distribution bring primary information on the evolution of those massive stars (e.g. Kochanek 2011).

While cool star winds readily form dust (see the review by Willson 2000), the intense radiation fields of young, massive stars would be expected to prevent dust formation in their circumstellar (CS) environment. However, dust is observed around some massive stars, for example in a subset of Car-

[1]Laboratoire Univers et Théories (CNRS/INSU, Observatoire de Paris, Université Paris Diderot), 5 place Jules Janssen, 92190 Meudon, France
contact email: mathieu.servillat@obspm.fr

[2]Laboratoire AIM (CEA/Irfu/SAp, CNRS/INSU, Universit Paris Diderot), CEA Saclay, Bat. 709, 91191 Gif-sur-Yvette, France

[3]Harvard University, Department of Astronomy, 60 Garden street, Cambridge, MA, 02138, USA

[4]AstroParticule et Cosmologie (Université Paris Diderot, CNRS/IN2P3, CEA/DSM, Observatoire de Paris, Sorbonne Paris Cité), 10 rue Alice Domon et Léonie Duquet, 75205 Paris Cedex 13, France

[5]Institut Universitaire de France, 103 Boulevard Saint-Michel, 75005 Paris, France

[6]European Southern Observatory, Karl Schwarzschild-Strasse 2, 85748 Garching bei München, Germany

bon Wolf-Rayet stars (WC) containing binaries with colliding winds (e.g. Crowther 2007), in luminous blue variables (LBVs) that show large dusty shells (see the review by Humphreys & Davidson 1994), or in supergiants showing the B[e] phenomenon (sgB[e], Zickgraf et al. 1986; Zickgraf 1998). sgB[e] stars are early-type stars with the simultaneous presence of low-excitation forbidden line emission and strong infrared excess in their spectra (Zickgraf 1998; Lamers et al. 1998). They share some observational properties with LBVs which are identified as luminous, hot, unstable supergiants that suffer irregular eruptions like S Dor and AG Car or more rarely giant eruptions like P Cyg and η Car (Humphreys & Davidson 1994). All those rare types of stars have in common a rapid mass loss in a dense wind and may represent some of the latest stages of the evolution of massive stars that lead to supernovae (SNe, e.g. Langer 2012).

It is not always clear whether those different classifications represent stars with different initial conditions, or stars at different evolutionary stages. It is however clear that dust can be formed around massive stars under specific conditions: strong stellar winds (responsible for high CS densities and thus shielding the dust grains from the stellar ionizing radiation), a high abundance of heavy elements (increasing the probability of dust formation), and clumping of the CS material (locally increasing the density). Those conditions are natural around massive ($> 20\ M_{\odot}$) and luminous ($> 10^5\ L_{\odot}$) objects, such as Wolf-Rayet stars, hot supergiants, and LBVs.

Another key parameter that could be related to the presence of CS dust around those massive stars may be binarity. Indeed, according to Sana et al. (2012), binary interaction dominates the evolution of massive stars : over 70% of all massive stars exchange mass with a companion, leading to a binary merger in one third of the cases. For sgB[e], it is suggested that the dust can be present in the outer parts of an equatorial disk, that probably forms through the bistability mechanism (Lamers & Pauldrach 1991) and possibly fast rotation (Bjorkman & Cassinelli 1993). Podsiadlowski et al. (2006) noticed that binary mergers produce an initially rapidly rotating merged object that is an excellent candidate for sgB[e] progenitors. Furthermore, Miroshnichenko (2007) proposed that sgB[e] and their low luminosity counterparts (FS CMa objects) are currently undergoing or have recently undergone a phase of rapid mass exchange in a binary system, associated with a strong mass loss and dust formation. Mass transfer in close binary systems with massive stars could then have an important role in shaping the structure of the diffuse CS environment (e.g. Plets et al. 1995; Millour et al. 2011).

In many cases, the inferred companion star could be much fainter than the massive primary and may have remained undetected. Among binary stars with a massive primary, high-mass X-ray binaries (HMXBs) are interesting test cases as the (pulsed) X-ray emission provides detailed information on the binary composition, orbital parameters and environment. Those may represent a new stage in the complex evolution of massive stars. In particular, a growing number of highly obscured HMXBs has been revealed by the *INTEGRAL* hard X-ray observatory (Matt & Guainazzi 2003; Filliatre & Chaty 2004; Walter et al. 2006; Chaty & Rahoui 2012; Coleiro & Chaty 2013, see also Chaty 2013 for a recent review). Those systems may harbour super or hypergiant stars in binaries with a compact object and enshrouded in a dense CS environment, probably hosting dust. We performed *Herschel* observations in the mid-infrared of six supergiant HMXBs in order to test the presence of dust and better understand its structure in those objects (see preliminary results in Chaty et al. 2013), and focus here on GX 301–2.

GX 301–2 is an obscured HMXB system consisting of an accreting neutron star fed by the stellar wind of a blue hypergiant (HG) B1 Ia$^+$ star (catalogued as Wray 977, or BP Cru, see e.g. Lewin et al. 1971; Jones et al. 1974; Kaper et al. 1995, 2006). The absorption varies from 10^{22} to 10^{24} atoms cm^{-2} (Mukherjee & Paul 2004) while the reddening is around $E(B-V)$=1.96 (Kaper et al. 2006). The system has an orbital period of $\sim$41.5 days with an eccentricity of 0.46 (Koh et al. 1997), and GX 301–2 is one of the slowest known pulsars with a period that slowly varied between 675 and 700 s (White et al. 1976; Pravdo et al. 1995; Evangelista et al. 2010). The magnetic field is around 4×10^{12} G, indicating a classical pulsar (Kreykenbohm et al. 2004). The X-ray mass function of the system has been estimated to be $\sim$31.9 $M_{\odot}$ (Sato et al. 1986), the highest

known for a HMXB with a pulsar companion, giving a mass of 43 ± 10 $M_\odot$ for the companion star and 1.85 ± 0.6 $M_\odot$ for the neutron star (Kaper et al. 2006). The X-ray light curve is characterized by bright flares occurring just before periastron passage of the neutron star (Watson et al. 1982). Those are clearly visible in the X-ray lightcurve[1] from the *Swift* Burst Alert Telescope (see Figure 1). The distance of GX 301–2 has been estimated to be 3.1 ± 0.64 kpc using a spectral energy distribution fitting procedure (Coleiro & Chaty 2013), consistent with the 3–4 kpc range proposed earlier (Kaper et al. 2006). Therefore the line of sight crosses the Southern Coalsack (e.g. Kaper et al. 2006) and passes through one or more spiral arms in our Galaxy, potentially contaminating the emission.

Kaplan et al. (2006) and Moon et al. (2007) studied the CS environment of the system and reported the presence of dust around the system through the detection of silicate absorption features and continuum components with low temperatures. However, they do not explore the geometry of this CS component. Moon et al. (2007) noticed the presence of low ionization potential forbidden emission lines, and discuss similarities with LBVs in the mid-infrared spectra.

In this paper we report on new *Herschel* observations of GX 301–2 (Section 2) and model the emission of the source in the wavelength domain from 0.4 to 4×10^4 μm in order to characterize the geometry of the CS environment. We detail the models used in Section 3, give the results of the fits to the data in Section 4 and discuss the properties and the possible geometries of the CS environment of GX 301–2 in Section 5.

2. Data acquisition and processing

We performed sensitive far-infrared (60–210 μm) observations[2] of GX 301–2 on 2011 August 2 with the ESA *Herschel* Space Observatory (Pilbratt et al. 2010), in particular employing *Herschel*'s large telescope and powerful science payload to do photometry using the PACS instrument (Poglitsch et al. 2010). At the date of the observations, the binary system was at its periastron, right after the periodic X-ray flare that can be seen in Figure 1. Observations were performed in the 3 available bands (blue 60-85 μm, green 85-130 μm and red 130-210 μm) in mini-scan map mode: medium speed, 10 scan legs of 2.5′ length with 2.0″ cross-scan step, with orientation angles at 70 and 110 degrees, and a repetition factor of 5 and 10 for each orientation angle for the blue/red and green/red filters respectively. This leads to a total integration time of 800, 1600 and 2400 s in the blue, green and red band, respectively.

The images are shown in Figure 2 where a point source corresponding to GX 301–2 can be seen in the center of the frame. The point source appears

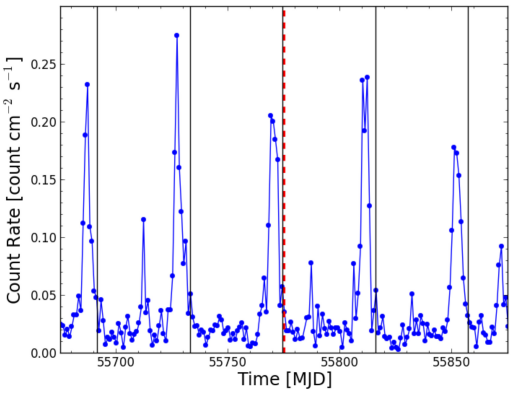

Fig. 1.— X-ray lightcurve of GX 301–2 with *Swift*/BAT (15–150 keV). The vertical lines indicate the periastron passages (based on Koh et al. 1997) and the red dashed vertical line the epoch of the *Herschel*/PACS observations on MJD 55775.05, right after periastron.

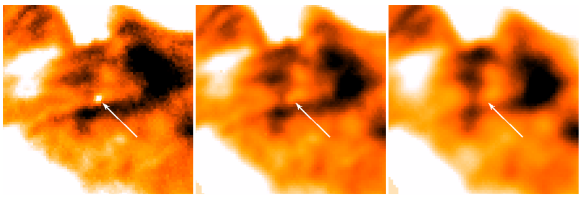

Fig. 2.— *Herschel*/PACS images centered on GX 301–2 (indicated by an arrow). From left to right, the blue, green and red bands are shown (70, 100 and 160 μm). The size of the snapshots is $2.5' \times 2.5'$, North is up, East is left.

[1] generated with the online tool on http://www.swift.ac.uk/ (Evans et al. 2007)

[2] The OBSIDs are 1342225124, 1342225125, 1342225126 and 1342225127

TABLE 1
FLUXES IN OPTICAL TO RADIO BANDS

Band name	Wavelength (μm)	Band width (μm)	Flux (Jy)	Flux error (Jy)	Note
B	0.441	0.102	0.034	0.012	Tycho-2, Høg et al. (2000)
V	0.551	0.089	0.206	0.014	Tycho-2, Høg et al. (2000)
J	1.242	0.240	3.28	0.07	2MASS, Skrutskie et al. (2006)
H	1.651	0.267	3.80	0.10	2MASS, Skrutskie et al. (2006)
Ks	2.166	0.282	3.59	0.07	2MASS, Skrutskie et al. (2006)
WISE-1*	3.353	0.663	0.47	···	Saturated, Wright et al. (2010)
IRAC-1	3.6	0.77	2.0	0.2	Kaplan et al. (2006)
IRAC-2	4.5	1.06	1.6	0.2	Kaplan et al. (2006)
WISE-2*	4.603	1.042	0.70	···	Saturated, Wright et al. (2010)
IRAC-3	5.8	1.43	1.16	0.12	Kaplan et al. (2006)
ISO-LW2*	6.75	···	0.837	···	Kaper et al. (2006)
IRAC-4	8.0	2.9	0.78	0.08	Kaplan et al. (2006)
MSX-A	8.28	3.36	0.63	0.07	Price et al. (2001)
AK09*	9.0	4.9	0.60	0.02	Ishihara et al. (2010)
ISO-LW10*	11.5	···	0.517	···	Kaper et al. (2006)
WISE-3	11.560	5.507	0.41	0.01	Wright et al. (2010)
MSX-C	12.13	1.72	0.45	0.05	Price et al. (2001)
MSX-D	14.65	2.23	0.32	0.03	Price et al. (2001)
AK18*	18.0	11.7	0.20	0.03	Ishihara et al. (2010)
WISE-4	22.088	4.101	0.22	0.01	Wright et al. (2010)
ISO-PHT3*	25	···	0.089	···	Kaper et al. (2006)
PACS-B	70	20	0.061	0.0066	This work
PACS-G	100	40	0.061	0.0149	This work
8.6 GHz	34860	600	0.72×10^{-3}	0.16×10^{-3}	Pestalozzi et al. (2009)

NOTE.—See the references in the text.
* Those points were not used in the modelling as they have lower precision (due to saturation, large bandwidth or large errors).

to be surrounded by an extended structure. Based on IRAS observations, Huthoff & Kaper (2002) suggested that the extended structure could be a wind bow-shock (see their Fig. 4). We further analyse the extended emission and possible cavity around GX 301–2 in a companion paper (Coleiro et al. in preparation).

We used HIPE (Ott 2010) to reprocess the data with custom scripts for PACS (M. Sauvage, private communication). The software *getsources* (Men'shchikov et al. 2012) was then used to detect the sources and filaments, and to extract fluxes using a multi-wavelength and multi-scale method. As the source is faint and the structure of the background complex, we masked the area outside a $2.4' \times 1.7'$ region around the target to avoid the presence of extended features seen at the edges of the images in Figure 2. We detected a point source at the position of GX 301–2 in the blue and green bands with fluxes of 61.0 ± 6.6 and 61.2 ± 14.9 mJy (with significances of 15.4 and 3.8 sigma respectively). No significant detection was made for the red band with a detection limit of 250 mJy at 3 sigma (note the presence of a close-by extended source blended with the point source).

The optical-infrared spectral energy distribution (SED) was completed using B and V-band magnitudes from the Tycho-2 catalog (Høg et al. 2000), and $JHKs$ magnitudes from the Two Micron All Sky Survey (2MASS, Skrutskie et al. 2006). We included fluxes at 3.6, 4.5, 5.8 and 8.0 μm from the Galactic Legacy Infrared Midplane Survey Extraordinaire (GLIMPSE) catalog based on observations with IRAC onboard *Spitzer* (Benjamin et al. 2003; Churchwell et al. 2009). As the central pixels of the source were saturated at 3.6 and 4.5 μm, we used the flux values estimated by Kaplan et al. (2006). We finally included fluxes at 12 and 22 μm obtained with the *Wide-field Infrared Survey Explorer* (WISE, Wright et al. 2010) and fluxes at 8.28, 12.13 et 14.65 μm obtained with the *Midcourse Space Experiment* (MSX, Price et al. 2001). The flux measurements from various observatories are reported in Table 1. Within the errors, the infrared measurements with different instruments are consistent. We thus used all these data simultaneously to characterize the emission of the source.

GX 301–2 was also observed at radio wavelengths (Pestalozzi et al. 2009) with ATCA (4.8 and 8.6 GHz) at 12 epochs spread between November 2008 and February 2009. Pestalozzi et al. (2009) found that the radio source showed a negative index during the X-ray outburst, and a positive index otherwise, though with large error bars. They suggest that the radio emission originates in two components: a persistent thermal emission from the wind of the HG mass donor Wray 977, and an episodic emission, perhaps a weak jet, that appears at the time of the X-ray outburst. The mean flux at 8.6 GHz when the source is detected is 0.72 ± 0.16 mJy. To estimate the flux due to the presence of strong winds around massive stars, we used Equation 4 in Scuderi et al. (1998) and input parameters estimated by Kaper et al. (2006) (i.e. a mass loss rate of $\dot{M} = 10^{-5}$ $M_\odot$ yr^{-1}, temperature $T = 18\,100$ K, and terminal velocity of the wind $v_{\rm inf} = 305$ km s^{-1}). We thus expect a 8.6 GHz flux of 2.5 mJy for GX 301–2. The discrepancy possibly indicates a lower mass-loss rate or larger distance, but the radio flux from a stellar wind can naturally vary by a factor of a few (Scuderi et al. 1998). During our *Herschel* observations, we can nevertheless expect free-free emission from the stellar wind, which may have some contribution to the mid-infrared emission down to $\sim$10 μm with a positive spectral index $\alpha = 0.6$ ($S_\nu \propto \nu^\alpha$, Wright & Barlow 1975).

3. Modeling the emission

The collected data allowed us to fit spectral models over five orders of magnitude, from 0.4 to 4×10^4 μm, with *Herschel* data in the 60–210 μm range bridging the gap between mid-infrared and radio observations for the first time for this kind of object.

We used the stellar photosphere model of Castelli & Kurucz (2004), hereafter CK04, and the stellar parameters derived by Kaper et al. (2006) for the star Wray 977 associated to GX 301–2 are: $T = 18\,100$ K, $\log(g) = 2.38$ and $R = 70$ $R_\odot$, for a distance $D = 3040$ pc. We thus selected the closest available CK04 model with $T = 18\,000$ K and $\log(g) = 2.5$ and kept the radius of the star fixed.

We also built an extinction law following Cardelli et al. (1989) in the visible, Indebetouw et al. (2005) between 1.25 and 8.0 μm, Lutz et al. (1996) between 8.0 and 24 μm and Moneti et al.

(2001) above 24 μm. The main parameter for the extinction law is the excess color $E(B-V)$. We adopt $R_V = A_V/E(B-V) = 3.1$ (see e.g. Savage & Mathis 1979). As the reddening is high for GX 301–2, the extinction law has a large impact on the shape of the SED. In particular, broad silicate absorption lines around 10 and 20 μm are visible and taken into account in the extinction law (Lutz et al. 1996). The obtained extinction law is particularly well suited for the case of GX 301–2, being largely based on observations in the Galactic Center and the Galactic plane. However, there could be local fluctuations of this law that are still not properly measured.

The optical-infrared SED of GX 301–2 has already been fitted between 1 and 10 μm by Kaplan et al. (2006), using two components: the star and a spherical black body emission with temperature 740 K and an extension $R_{dust} = 9 \times R_{star}$ to model the surrounding dust. Using Spitzer data up to 38 μm, Moon et al. (2007) found that multiple emission components were required to model the continuum emission of the dust (a hot component with $T \sim 700$ K and a warm component with $T \sim 180$ K).

In order to constrain the geometry of the CS environment, we considered several models that could explain the infrared excess found in this source: (i) a power law spanning several orders of magnitude, (ii) spherical black body dust components (as in Kaplan et al. 2006 and Moon et al. 2007), (iii) disk-like dust components. For (ii) and (iii), we also tested the addition of a power law with a fixed spectral index $\alpha = 0.6$ and the observed flux at 8.6 GHz in order to model the free-free emission from the stellar wind detected by Pestalozzi et al. (2009).

GX 301–2 appears to be similar to two obscured X-ray binary systems hosting a sgB[e] star: IGR J16318-4848 (Revnivtsev et al. 2003; Filliatre & Chaty 2004; Kaplan et al. 2006; Moon et al. 2007; Chaty & Rahoui 2012) that present a circumstellar disk with dust, and XTE J0421+560 (CI Cam) for which IRAS 12–100 μm data suggested the existence of a substantial circumstellar dust shell (Belloni et al. 1999; Clark et al. 1999). We thus investigate the possibility of having a similar distribution of dust as a disk surrounding the hyper giant star, as it is generally observed for sgB[e]. Lamers et al. (1998) pointed out that the CS envelope geometry is most probably disk-like for those stars, which naturally provides conditions for a high density of the CS material and, as a consequence, for shielding of CS dust from the ionizing stellar radiation. We thus used a similar model to the one proposed by Chaty & Rahoui (2012) for IGR J16318-4848, initially based on the dust structure of Herbig Ae/Be stars (Monnier et al. 2005). The CS environment of those objects is well described as a simple disk model possessing a central optically thin (dust-free) cavity, ringed by hot dust — a rim — emitting at the expected sublimation temperature ($\sim$1 500 K), hereafter called a *rimmed disk*. For some systems, however, the inner gas in the mid-plane may be optically thick, partially shielding the innermost dust from stellar radiation and causing the dust sublimation radius to shrink for the same sublimation temperature. This would correspond to a *classical disk* model.

We assumed that the disk is completely flat with a ring-like rim of constant temperature $T_{\rm rim}$, located at an inner radius $R_{\rm in}$ and of width $H_{\rm rim}$, as in Lachaume et al. (2007). The equation used to model the flux can therefore be written as follows:

$$\begin{aligned} F_\nu(\nu) &= \left(\frac{R_*}{D}\right)^2 \times \mathrm{CK04}(\nu, T_*) \\ &+ 2\pi \frac{H_{\rm rim} R_{\rm in}}{D^2} \cos(i) B(\nu, T_{\rm rim}) \\ &+ 2\pi \frac{\cos(i)}{D^2} \int_{R_{\rm in}}^{R_{\rm out}} r B(\nu, T(r)) \mathrm{d}r \quad (1) \end{aligned}$$

where T_*, R_* et D are respectively the temperature, the radius and the distance of the companion star, and CK04 is the stellar photosphere model (Castelli & Kurucz 2004). $B(\nu, T)$ is the Planck function at the frequency ν. The disk is defined by i, $T_{\rm in}$, $R_{\rm out}$ which are respectively the inclination of the disk, the temperature at the inner radius $R_{\rm in}$, and the outer radius. $T(r) = T_{\rm in}\,(r/R_{\rm in})^{-q}$ is the disk temperature at a given radius r where q is a dimensionless parameter generally ranging from 0.5 to 0.75 (irradiated to viscous disc, Chiang & Goldreich 1997).

We fixed the inclination to 60° as estimated by Kaper et al. (2006) for the inclination of the binary system, assuming that the inclination of a disk around the companion star would be similar. We only considered the case of a viscous disk

($q = 0.75$), as expected for this kind of system (e.g. Okazaki 2007). It is clear from Equation 1 that we expect degeneracies in the fits between the radii R_*, $R_{\rm in}$ and the distance D, so the absolute value of those parameters should be taken with care. There is also a degeneracy between $H_{\rm rim}$ and $R_{\rm in}$, we thus arbitrarily fixed $H_{\rm rim}$ to 15 $R_\odot$ following the results of Chaty & Rahoui (2012).

4. Fit results

We report the results of the SED fitting in Table 2 and plot the data and models in Figures 3 to 6.

We first tried to fit a power law in addition to the CK04 stellar photosphere model (and including the extinction law). We found a statistically acceptable fit with an index $\alpha = 0.75 \pm 0.01$ (see Table 2). This index is different from the 0.6 expected for stellar winds (Wright & Barlow 1975). There is a deviation from the model in one *Herschel* energy band (accounting for most of the χ^2 excess, see Figure 3) that may indicate a marked curvature in the spectrum, and the necessity to explore more complex models.

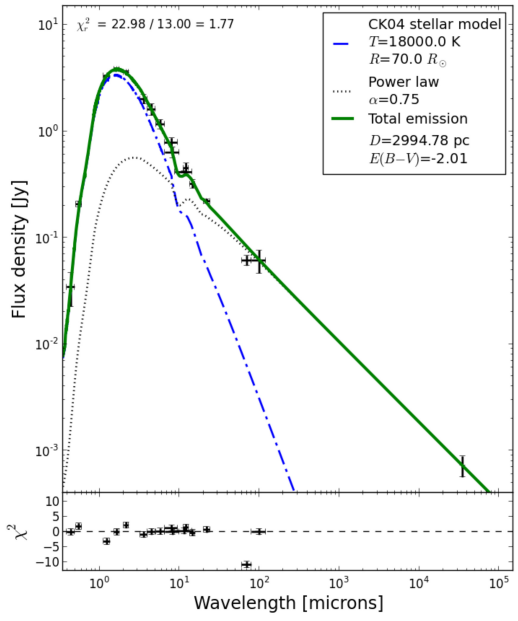

Fig. 3.— SED of GX 301–2 (Wray 977) fitted with a stellar photosphere model and a power law to account for the infrared excess.

In order to account for the presence of dust around the system (see Moon et al. 2007), we fitted a spherical black-body component (as in Kaplan et al. 2006) instead of the power law and found a low temperature $T_s = 411 \pm 47$ K and radius $R_s = 1288 \pm 197$ $R_\odot$ (see Figure 4, left). We note that the *Herschel*/PACS data points are well above the model, resulting in a reduced χ^2 of 3.95 with 12 degrees of freedom. We obtained a slightly lower temperature in our fit compared to Kaplan et al. (2006). Following Moon et al. (2007), we fixed all the parameters and added a second black-body component to account for this mid-infrared excess. We found a low temperature of 70 K and rather large radius of ∼6000 $R_\odot$ for this second component. If we thaw the parameters and add instead a component from the stellar wind corresponding to the observed radio flux and with a spectral index of $\alpha = 0.6$, the reduced χ^2 is improved to 2.16, with a similar temperature and slightly smaller radius (see Figure 4, right). Given the low number of degrees of freedom in our fits, the standard deviation from the expected reduced χ^2 of 1 is large. Using Gaussian approximation, the width of the χ^2 distribution would be 0.4, but it is likely larger in our case (see e.g. Andrae et al. 2010). The reduced χ^2 we obtained for models presented in Figure 4 are thus barely acceptable in theory but cannot be completely ruled out. We note that there is a large spread in the residuals for the $JHKs$ bands, and indication of a different curvature than the proposed model (dominated by the stellar photosphere model and the extinction law in those bands).

We then used a classical viscous disk model (as described in Section 3) in addition to the CK04 model and obtained acceptable fits (see Figure 5 and Table 2). The inner temperature of the disk is consistent with the dust sublimation temperature (∼1 500 K). The addition of a power law corresponding to the stellar wind slightly improved the fit and drastically changed the extension of the disk from $R_{\rm out} \sim 4200$ to 1800 $R_\odot$. This would correspond to ∼25 stellar radii, or ∼8 AU. With this model, the residuals for the $JHKs$ bands are not improved. At the outer edge of this classical disk, the temperature drops to ∼150 K.

Finally, we fitted the SED with the rimmed disk model defined in Equation 1 (see Section 3) and report the results in Figure 6 and Table 2. We ob-

TABLE 2
FIT RESULTS

Model	D (pc)	$E(B-V)$	$T_{\rm in}$ (K)	$R_{\rm in}$ ($R_\odot$)	$R_{\rm out}$ ($R_\odot$)	$T_{\rm rim}$ (K)	α	χ^2/dof
Power law	2994±54	2.01±0.04	–	–	–	–	0.75±0.01	23.0/13
Sphere	2888±62	2.08±0.06	411±47	–	1288±197	–	–	47.4/12
	2950±48	2.06±0.04	470±69	–	919±169	–	[0.6]	25.9/12
Classical disk	2784±42	2.05±0.04	1658±127	[70]	4263±1437	–	–	21.4/12
	2830±42	2.04±0.04	1711±150	[70]	1785±623	–	[0.6]	18.6/12
Rimmed disk	2961±95	1.97±0.05	238±35	3275±817	4208±802	1837±306	–	14.1/10
	3215±405	1.92±0.09	400±95	1129±419	1858±339	3267±1672	[0.6]	8.4/10

NOTE.—The parameters reported here are defined is section 3. The star temperature $T_* = 18\,000$ K, and radius $R_* = 70\ R_\odot$ are fixed parameters. When other parameters are fixed, we indicate the value in brackets. $R_{\rm rim}$ is equal to $R_{\rm in}$ and $H_{\rm rim}$ is fixed to 15 $R_\odot$ following Chaty & Rahoui (2012). The inclination is fixed to $i = 60^\circ$ (Kaper et al. 2006).

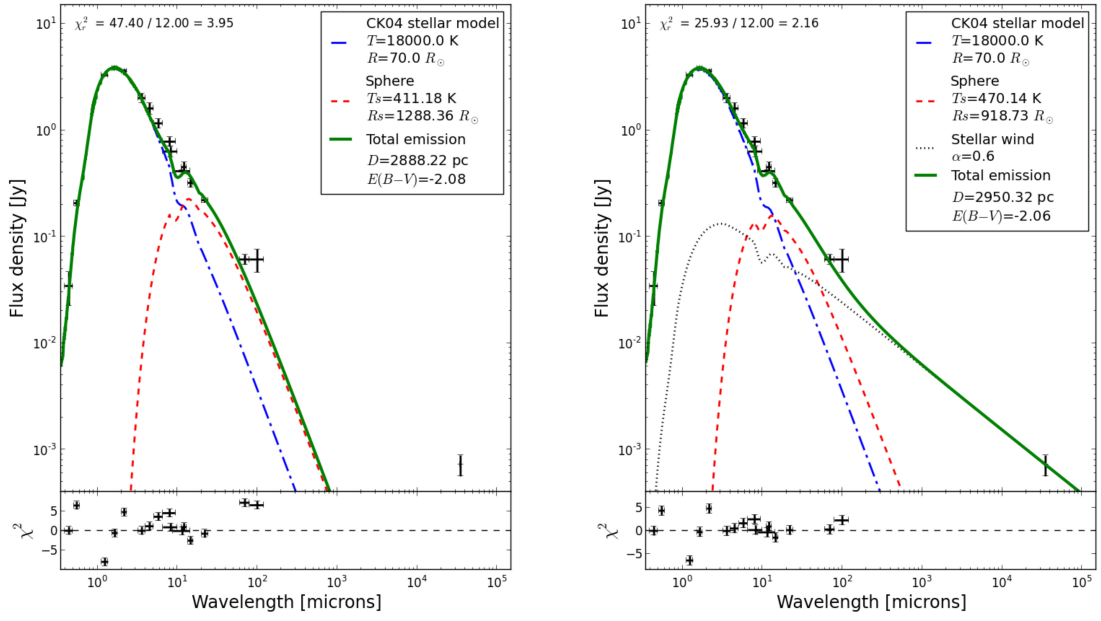

Fig. 4.— SED of Wray 977 (GX 301–2) fitted with a stellar photosphere model and a spherical black-body component (left) and an additive power-law to account for the stellar wind (right).

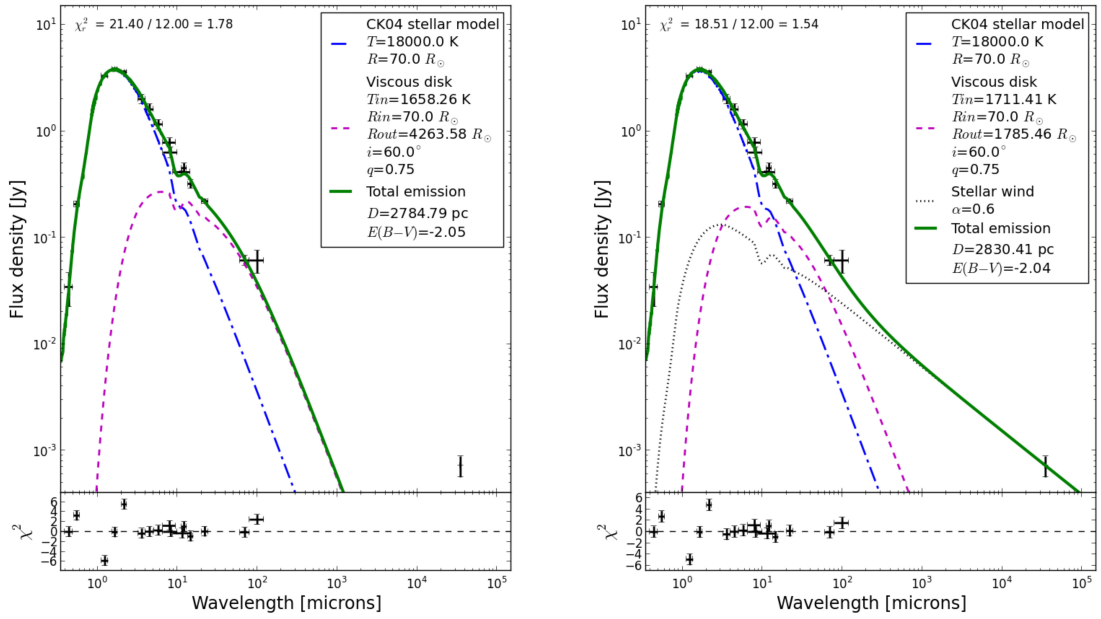

Fig. 5.— SED of Wray 977 (GX 301–2) fitted with a stellar photosphere model and a classical disk component (left) and an additive power-law to account for the stellar wind (right).

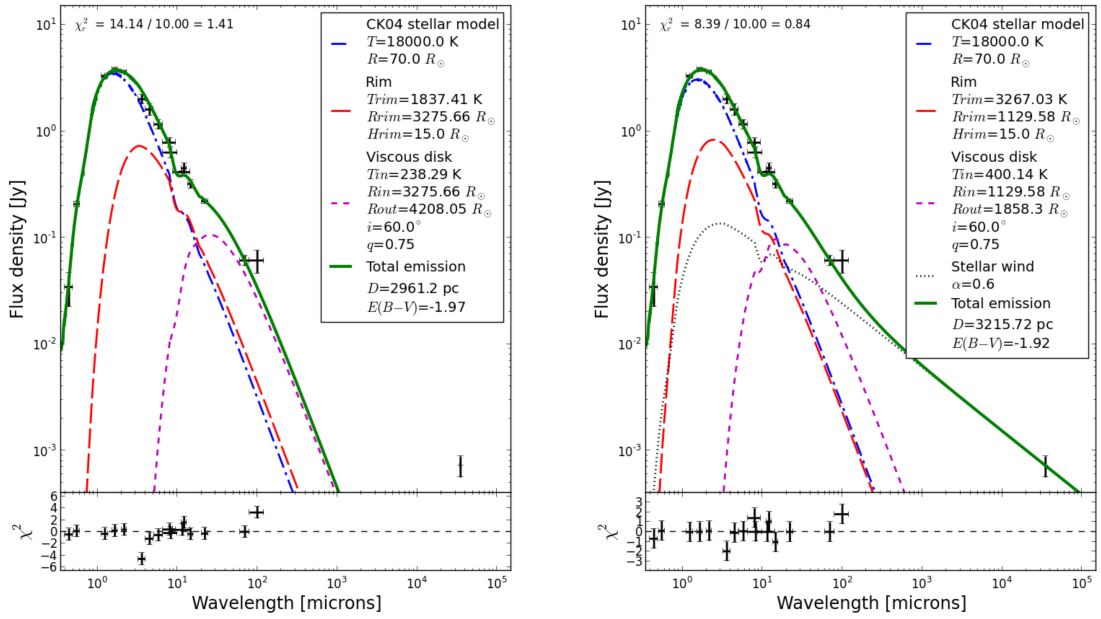

Fig. 6.— SED of Wray 977 (GX 301–2) fitted with a stellar photosphere model and a rimmed disk component (left) and an additive power-law to account for the stellar wind (right).

tained the best fits with this model and, in particular, flatter residuals for the $JHKs$ bands thanks to the rim component that dominates the contribution to the near-infrared excess. The temperature of the rim is consistent with the dust sublimation temperature as expected for this kind of model (see Section 3 and Monnier et al. 2005). The addition of a power law component (stellar wind) again drastically changed the extension of the disk, to reach a similar value to that found for the classical disk, around 1800 $R_\odot$. At the outer edge of this rimmed disk, the temperature drops to ∼250 K.

5. Discussion

Using all the available visible-infrared photometry on GX 301–2, with the addition of *Herschel* and radio data points for the first time, we fitted spherical and disk-like dust/gas distribution models. We globally found the same reddening, $E(B-V) \sim 2.0$, and a similar distance, $D \sim 3.0$ kpc, with all the different models. This is consistent with previously reported values (Coleiro & Chaty 2013; Kaper et al. 2006). As the stellar radius was fixed to the most likely value found by Kaper et al. (2006), the distance is not totally constrained and may be slightly different than the values presented in Table 2.

The addition of a power law, used to model the free-free emission from the stellar wind around the HG and detected in radio by Pestalozzi et al. (2009), clearly improved the fits for all models. It thus seems likely that this component is required and has some contribution to the mid-infrared flux from the source. This contribution could even dominate the 70 μm flux (see Figures 5 and 6, right). Such a free-free emission component has been proposed by Kaper et al. (2006), but ruled out by Kaplan et al. (2006) and thus required confirmation.

5.1. Structure of the CS environment

The model components related to the infrared excess are indicative of the structure of the CS environment of GX 301–2.

We obtain a relatively good fit over five orders of magnitude in wavelength with the simplest model composed of the CK04 stellar photosphere model and a power-law with index ∼0.75 (with an appropriate extinction law). Such a high index is not ruled out by Pestalozzi et al. (2009) in the radio range, as their error bars are large, but this index is not consistent with a spherical wind model (index of 0.6 expected). The global indices from radio to infrared found for similar stars such as P Cyg seem to reach such a high value. This may indicate a more complex wind structure, however, a break between radio and near-infrared is clearly possible, with a radio power law index closer to 0.6 and a higher index in the infrared for those objects (Wright & Barlow 1975). A non-spherical geometry would produce a more flattened radio spectrum. Higher indices could be the consequence of a lower ionized gas fraction, involving the presence of neutral condensations and possibly the presence of CS dust (Wright & Barlow 1975).

It thus seems that the infrared excess in the SED might be explained mostly by the stellar wind. However, there is a number of features that point towards more complex models. First, this simple model would contradict the idea that this highly obscured source hosts dust in its CS environment, as revealed by intrinsic silicate absorption lines and continuum emission excess in the infrared (see e.g. Kaplan et al. 2006; Moon et al. 2007). The *Herschel*/PACS data point at 70 μm appears to be more than 3σ away from the model, suggesting a curvature in the spectrum. Also, the curvature of the data in $JHKs$ is not well followed by the model (see residuals in Figure 3). We thus cannot exclude a break in the mid-infrared with a change of index of the power law slope, or discontinuities as discussed in Wright & Barlow (1975). More data points would be required in order to better constrain the shape of the SED.

We thus give credit to more explicit models that are used to test the possible geometry of the CS gas/dust. The spherical distribution models lead to lower fit quality, though they cannot be completely ruled out. The fits of disk models returned relevant parameter values, though we note that degeneracies in the fits and a complex extended emission around the source might bring additional uncertainties on the absolute values reported here. The size of the dusty disks we derived is about 1 800 $R_\odot$, (25 stellar radii, or 8 AU) which is comparable to the sizes derived by Lachaume et al. (2007) for the B[e] star Hen 3–1191 or derived through interferometry for similar objects (Mil-

lour et al. 2011). Compared to the dusty shells observed among most of LBVs (up to a few pc, Clark et al. 2003), the size is however much smaller. The low temperatures we obtained in the disk, which are close to 200 K at the outer edges of the disk, are well below the dust sublimation temperature, indicating that dust can indeed be formed in such a CS environment of GX 301–2.

The rimmed disk model is particularly instructive on the possible structure of the CS environment. It contains an irradiated rim at the inner edge of the disk that efficiently protects the disk from the ionizing radiation of the star. Following Lachaume et al. (2007), the rim radius $R_{\rm rim}$ for a temperature close to the dust sublimation temperature is expected to be around 1 400 $R_\odot$ for GX 301–2 in the large gap scenario (their Equation 2, valid for a rimmed disk with optically thin inner gas), which corresponds to the value obtained in our final fit (Figure 6, right). There is a clear degeneracy between $R_{\rm rim}$ and $H_{\rm rim}$ (the latter is fixed in the model). Therefore we cannot give clear constraints to the value of $R_{\rm rim}$. In the small gap scenario (more similar to a classical disk with optically thick inner gas, see Lachaume et al. 2007), the radius at which the temperature equals the dust sublimation temperature is expected to be $\sim$400 $R_\odot$. However, such temperatures are found at the inner edge of the classical disk in our modelling, close to the star surface (thus significantly below 400 $R_\odot$), arguing against the classical disk model.

For sgB[e] stars, it is generally agreed that a rimmed disk is present around the star, but strong [O I] emission lines detected in their NIR spectra rather points towards a temperature between 5 000 and 10 000 K for the rim (Kraus et al. 2007). In GX 301–2, there are no such lines, and thus, a rim at such a high temperature cannot be present. Therefore, the rimmed disk solution we obtained, with a rim temperature compatible with the dust sublimation temperature, appears to be plausible.

The size of the dusty disk structure is larger than the neutron star distance to the HG star in GX 301–2, estimated to be 100–200 $R_\odot$, so about twice the stellar radius (e.g. Kaper et al. 2006). The structure we observe here would thus surround the binary system. The possible presence of a gas stream close to the periastron of the orbit of the neutron star has been proposed to explain the evolution of the accretion rate, as seen in X-rays (Leahy 2002; Evangelista et al. 2010). Such a feature would thus not be directly connected, at least spatially, to the CS dusty disk.

5.2. Comparison with similar objects

Globally, the CS environment of GX 301–2 appears to be similar to the environment of the obscured HMXB IGR J16318–4848 hosting a sgB[e] companion star (Chaty & Rahoui 2012) and to sgB[e] stars in general. We thus strengthen the connections between the two systems, that may have undergone a similar evolution that led to the formation of a dense CS environment with a disk hosting dust. GX 301–2 has known orbital parameters, in particular a significant eccentricity, while there is no evidence for variability for IGR J16318–4848 and most probably a circular orbit. This difference might be due to a slightly different stage in the evolution after the supernova that formed the neutron star, or to a different initial mass or conditions in the system.

For another similar source, CI Cam, the geometry of the dusty envelope has been unambiguously determined with long baseline optical interferometry as a torus or a disc (of a few AU in radius) and the hypothesis of a spherical dust shell is totally ruled out (Thureau et al. 2009). The binary companion would also lie interior to the dusty disc. This structure is similar to the proposed rimmed disk model we tested for GX 301–2.

GX 301–2 has been reported to share common properties with 4U 1907+097, which is also a slow pulsar and a O8/O9 supergiant companion with a dense stellar wind (Cox et al. 2005). It seems to follow a similar evolution track. This system is a highly obscured HMXB and could be a missing link between supergiant fast X-ray transients (SFXTs) and ordinary accreting pulsars (Doroshenko et al. 2012). It would be interesting to test the presence of surrounded dust around the system, however, its larger distance and high extinction make it more difficult to study.

More globally, IGR J16318–4848 is the prototype of a larger class of obscured X-ray binaries, and as such, this whole class of objects could represent a similar step in the evolution of massive stars in binary systems. The number of known supergiant HMXBs has dramatically increased over

the last decade with new detections using *INTEGRAL*. For the HMXBs confirmed by spectral type we now have 49% of Be HMXBs, 42% of supergiant HMXBs and 9% of peculiar HMXBs (Coleiro et al. 2013), while we had only 4% of supergiant HMXBs before *INTEGRAL*. Obscured systems hosting a supergiant may be explained by ejections of matter during phases of interaction with the compact object (see e.g. Kraus et al. 2010; Wheelwright et al. 2013). This scenario might be related to the formation of a dusty disk around those systems. More observations and modeling of their infrared excess, and possibly mapping of the CS environment through interferometry, would reveal and confirm the similarities of those objects and allow us to perform population studies.

5.3. Origin of the dusty disk

Assuming that a disk of material effectively surrounds GX 301–2, it might have initially formed through the bi-stability mechanism, a scenario proposed for sgB[e] stars (Lamers & Pauldrach 1991; Pauldrach & Puls 1990). This is strengthened by the fact that the surface effective temperature found for the HG star in GX 301–2 is close to 19 300 K, and was probably higher before its evolution to the HG stage. With this mechanism it is possible to get a density contrast of about 10 between the equator and the pole. Another scenario proposed for the formation of a disk in sgB[e] system requires a high rotational velocity, leading to the formation of an equatorial, wind compressed disk (Bjorkman & Cassinelli 1993; Bjorkman 1999). This scenario might be complementary to the bi-stability mechanism, as shown by Pelupessy et al. (2000) in order to explain the formation of disks around sgB[e] with observed density contrast of a factor $\sim$100.

In addition to those processes, the presence of a close-by companion (the neutron star in GX 301–2), even when it is much less massive than the primary, could drastically affect a stellar wind. It was argued that the formation of a dusty disk could be directly due to the presence of a companion around the massive star and non-conservative mass tranfer (Plets et al. 1995; Clark et al. 2013). Tidal interaction in the binary system could create high density blobs, that would form a rim. This rim could then efficiently protect the disk from the stellar radiation, and enable the formation of dust. The fact that we favour a rimmed disk model for GX 301–2 appears to give credit to this scenario. In the same way, some sgB[e] exhibit a disk and the most probable hypothesis is that the accumulation of matter in the equatorial plane is due to the presence of a low mass companion (e.g. Millour et al. 2011, 2013).

5.4. Evolutionary track

The evolution of the particular system GX 301–2 has been modeled by Wellstein & Langer (1999) who favoured a scenario with an initial binary system of 25 and 26 $M_{\odot}$, that underwent conservative mass transfer. The associated transfer of angular momentum has led to the formation of one of the slowest known pulsar with a wide orbit. It also potentially spun up the HG star, possibly enabling, or strengthening, the mechanism of disk formation around the HG star. The possible future evolution of the system has been modelled by Belczynski et al. (2012), as GX 301–2 is a potential progenitor for a black hole + neutron star binary, and thus among the most promising gravitational wave sources. However, the expansion of the massive companion will be so rapid that the system will probably create a Wolf-Rayet (WR), and then end up with the neutron star sinking into the helium core of the companion star, i.e. a merger.

The disk-like structure of the dust around the HG in GX 301–2 is strikingly similar to the structure observed around supergiant stars showing the B[e] phenomenon (Lamers et al. 1998), suggesting a link between those two classes of objects. We also note that GX 301–2 (Wray 977) has similar properties to the group of LBV stars (Clark et al. 2012, 2013), also suggesting a connection between those classes. It thus appears that there are probably evolutionary links between the HG stage in GX 301–2, sgB[e] systems, LBVs, and obscured HMXBs.

Forbidden lines have been detected in GX 301–2 (Moon et al. 2007), though there are differences with the lines more commonly associated to the B[e] phenomenon. The inferred temperature for the radiation exciting the [Ne II] and [Ne III] lines is hotter than the stellar photospheres, so there can be some contribution from the illumination of hard X-rays from the central compact X-ray

source (Moon et al. 2007). As [Ni II] and [Fe II] were detected only in IGR J16318–4848 (that contains a sgB[e]) while [Fe III] was only in GX 301–2, this suggests the presence of a slightly harder radiation field in GX 301–2. One possibility is that the HG stage is similar to the sgB[e] stage for systems with a harder radiative field (e.g. hosting an X-ray source), or that are more massive initially. It is however more likely that the HG is an evolved sgB[e] (sgB[e] → HG) as it now presents a similar CS environment, but a lower stellar effective temperature and larger radius. As such, a rimmed disk as the one we modeled could be the remnant of an initial sgB[e] disk, with a lower rim temperature, following the lower stellar temperature.

As LBVs generally show large dusty shells that are not observed around GX 301–2, the evolutionary sequence can only be HG → LBV, if there is indeed an evolutionary link. Clark et al. (2012) noticed that blue HG yielded physical properties intermediate between blue supergiants and LBVs, such as mass loss rate, wind velocity, stellar luminosity and temperature. All this suggests that blue HGs are the immediate descendants of blue supergiants and progenitors of LBVs, for initial masses in the range ∼30–60 $M_{\odot}$.

GX 301–2 might represent a peculiar and short-lived stage in the evolution of massive stars in binary systems, that could be represented by the following steps:

$$\text{sgB[e]} \rightarrow \text{HG} \rightarrow \text{LBV} \rightarrow \text{WR} \rightarrow \text{SN}$$

This track might be specific to binary systems that become X-ray binaries with an accreting compact object during their evolution, and can be seen as highly obscured X-ray binaries at one point.

6. Conclusions

We modeled the optical to radio spectral energy distribution of GX 301–2 and found relatively good fits with different models, all containing a stellar photosphere model and a power law representing the stellar wind. These two components could be sufficient to explain the emission, though they do not explain the presence of dust as reported in previous work. Models including a spherical or disk-like distribution of material can also reproduce the spectral energy distribution. Through comparisons with similar objects, the spherical and classical disk distribution seem less likely to be present in GX 301–2. The rimmed disk model shows acceptable parameters, and relates to viable mechanisms that would explain the evolution of the system as well as strengthen the connections to other categories of massive stars such as LBVs and sgB[e].

We thank the referee for his input and interesting comments. MS acknowledges founding from the Centre National dEtudes Spatiales (CNES). This work is based on observations obtained with MINE – the Multi-wavelength INTEGRAL NEtwork –, supported by the CNES. This research made use of Astropy, a community-developed core Python package for Astronomy (Astropy Collaboration et al. 2013). This research has made use of the SIMBAD database, operated at CDS, Strasbourg, France. PACS has been developed by a consortium of institutes led by MPE (Germany) and including UVIE (Austria); KU Leuven, CSL, IMEC (Belgium); CEA, LAM (France); MPIA (Germany); INAF- IFSI/OAA/OAP/OAT, LENS, SISSA (Italy); IAC (Spain). This development has been supported by the funding agencies BMVIT (Austria), ESA-PRODEX (Belgium), CEA/CNES (France), DLR (Germany), ASI/INAF (Italy), and CICYT/MCYT (Spain).

Facilities: Herschel.

REFERENCES

Andrae, R., Schulze-Hartung, T., & Melchior, P. 2010, arXiv:1012.3754

Astropy Collaboration, et al. 2013, A&A, 558, 33

Belczynski, K., Bulik, T., & Fryer, C. L. 2012, arXiv:1208.2422

Belloni, T., et al. 1999, ApJ, 527, 345

Benjamin, R. A., et al. 2003, PASP, 115, 953

Bjorkman, J. E. 1999, Variable and Non-spherical Stellar Winds in Luminous Hot Stars, 523, 120, (c) 1999: Springer-Verlag

Bjorkman, J. E., & Cassinelli, J. P. 1993, ApJ, 409, 429

Cardelli, J. A., Clayton, G. C., & Mathis, J. S. 1989, ApJ, 345, 245

Castelli, F., & Kurucz, R. L. 2004, arXiv, 5087

Chaty, S. 2013, ASR, 52, 2132, COSPAR

Chaty, S., Coleiro, A., Servillat, M., Heras, J. A. Z., & Rahoui, F. 2013, In: An INTEGRAL view of the high-energy sky (the first 10 years), Proceedings of Science, INTEGRAL (2012), 092 (arXiv:1302.4194)

Chaty, S., & Rahoui, F. 2012, ApJ, 751, 150

Chiang, E. I., & Goldreich, P. 1997, ApJ, 490, 368

Churchwell, E., et al. 2009, PASP, 121, 213

Clark, J. S., Bartlett, E. S., Coe, M. J., Dorda, R., Haberl, F., Lamb, J. B., Negueruela, I., & Udalski, A. 2013, A&A, 560, 10

Clark, J. S., Egan, M. P., Crowther, P. A., Mizuno, D. R., Larionov, V. M., & Arkharov, A. 2003, A&A, 412, 185

Clark, J. S., Najarro, F., Negueruela, I., Ritchie, B. W., Urbaneja, M. A., & Howarth, I. D. 2012, A&A, 541, 145

Clark, J. S., Steele, I. A., Fender, R. P., & Coe, M. J. 1999, A&A, 348, 888

Coleiro, A., & Chaty, S. 2013, ApJ, 764, 185

Coleiro, A., Chaty, S., Heras, J. A. Z., Rahoui, F., & Tomsick, J. A. 2013, A&A, 560, 108

Cox, N. L. J., Kaper, L., & Mokiem, M. R. 2005, A&A, 436, 661

Crowther, P. A. 2007, ARA&A, 45, 177

Doroshenko, V., Santangelo, A., Ducci, L., & Klochkov, D. 2012, A&A, 548, 19

Evangelista, Y., et al. 2010, ApJ, 708, 1663

Evans, P. A., et al. 2007, A&A, 469, 379

Filliatre, P., & Chaty, S. 2004, ApJ, 616, 469

Heger, A., Fryer, C. L., Woosley, S. E., Langer, N., & Hartmann, D. H. 2003, ApJ, 591, 288

Høg, E., et al. 2000, A&A, 355, L27

Humphreys, R. M., & Davidson, K. 1994, Astronomical Society of the Pacific, 106, 1025

Huthoff, F., & Kaper, L. 2002, A&A, 383, 999

Indebetouw, R., et al. 2005, ApJ, 619, 931

Ishihara, D., et al. 2010, A&A, 514, 1

Jones, C. A., Chetin, T., & Liller, W. 1974, ApJ, 190, L1

Kaper, L., Lamers, H. J. G. L. M., Ruymaekers, E., van den Heuvel, E. P. J., & Zuiderwijk, E. J. 1995, A&A, 300, 446

Kaper, L., van der Meer, A., & Najarro, F. 2006, A&A, 457, 595

Kaplan, D. L., Moon, D.-S., & Reach, W. T. 2006, ApJ, 649, L107

Kochanek, C. S. 2011, ApJ, 743, 73

Koh, D. T., et al. 1997, ApJ, 479, 933

Kraus, M., Borges Fernandes, M., & Chesneau, O. 2010, In: Binaries - Key to Comprehension of the Universe, Eds Andrej Prsa and Miloslav Zejda, ASPC, 435, 395

Kraus, M., Fernandes, M. B., & de Araújo, F. X. 2007, A&A, 463, 627

Kreykenbohm, I., Wilms, J., Coburn, W., Kuster, M., Rothschild, R. E., Heindl, W. A., Kretschmar, P., & Staubert, R. 2004, A&A, 427, 975

Lachaume, R., Preibisch, T., Driebe, T., & Weigelt, G. 2007, A&A, 469, 587

Lamers, H. J. G., & Pauldrach, A. W. A. 1991, A&A, 244, L5

Lamers, H. J. G. L. M., Zickgraf, F.-J., de Winter, D., Houziaux, L., & Zorec, J. 1998, A&A, 340, 117

Langer, N. 2012, ARA&A, 50, 107

Leahy, D. A. 2002, A&A, 391, 219

Lewin, W. H. G., McClintock, J. E., Ryckman, S. G., & Smith, W. B. 1971, ApJ, 166, L69

Lutz, D., et al. 1996, A&A, 315, L269

Matt, G., & Guainazzi, M. 2003, MNRAS, 341, L13

Men'shchikov, A., André, P., Didelon, P., Motte, F., Hennemann, M., & Schneider, N. 2012, A&A, 542, 81

Millour, F., Meilland, A., Chesneau, O., Stee, P., Kanaan, S., Petrov, R., Mourard, D., & Kraus, S. 2011, A&A, 526, 107

Millour, F., Meilland, A., Stee, P., & Chesneau, O. 2013, The Environments of the Sun and the Stars, Lecture Notes in Physics, 857, 149, Springer-Verlag Berlin Heidelberg (ISBN 978-3-642-30647-1)

Miroshnichenko, A. S. 2007, ApJ, 667, 497

Moneti, A., Stolovy, S., Blommaert, J. A. D. L., Figer, D. F., & Najarro, F. 2001, A&A, 366, 106

Monnier, J. D., et al. 2005, ApJ, 624, 832

Moon, D.-S., Kaplan, D. L., Reach, W. T., Harrison, F. A., Lee, J.-E., & Martin, P. G. 2007, ApJ, 671, L53

Mukherjee, U., & Paul, B. 2004, A&A, 427, 567

Okazaki, A. T. 2007, In: Active OB-Stars: Laboratories for Stellar and Circumstellar Physics, ASP Conf. Ser., 361, 230

Ott, S. 2010, ADASS XIX, ASP Conf. Series, 434, 139

Pauldrach, A. W. A., & Puls, J. 1990, A&A, 237, 409

Pelupessy, I., Lamers, H. J. G. L. M., & Vink, J. S. 2000, A&A, 359, 695

Pestalozzi, M., Torkelsson, U., Hobbs, G., & López-Sánchez, Á. R. 2009, A&A, 506, L21

Pilbratt, G. L., et al. 2010, A&A, 518, L1

Plets, H., Waelkens, C., & Trams, N. R. 1995, A&A, 293, 363

Podsiadlowski, P., Morris, T. S., & Ivanova, N. 2006, Stars with the B[e] Phenomenon. ASP Conference Series, 355, 259

Poglitsch, A., et al. 2010, A&A, 518, L2

Pravdo, S. H., Day, C. S. R., Angelini, L., Harmon, B. A., Yoshida, A., & Saraswat, P. 1995, ApJ, 454, 872

Price, S. D., Egan, M. P., Carey, S. J., Mizuno, D. R., & Kuchar, T. A. 2001, AJ, 121, 2819

Revnivtsev, M. G., Sazonov, S. Y., Gilfanov, M. R., & Sunyaev, R. A. 2003, AstL, 29, 587

Sana, H., et al. 2012, Science, 337, 444

Sato, N., Nagase, F., Kawai, N., Kelley, R. L., Rappaport, S., & White, N. E. 1986, ApJ, 304, 241

Savage, B. D., & Mathis, J. S. 1979, In: Annual review of astronomy and astrophysics, ARA&A, 17, 73 (A79-54126 24-90)

Scuderi, S., Panagia, N., Stanghellini, C., Trigilio, C., & Umana, G. 1998, A&A, 332, 251

Skrutskie, M. F., et al. 2006, AJ, 131, 1163

Thureau, N. D., et al. 2009, MNRAS, 398, 1309

Walter, R., et al. 2006, A&A, 453, 133

Watson, M. G., Warwick, R. S., & Corbet, R. H. D. 1982, MNRAS, 199, 915

Wellstein, S., & Langer, N. 1999, A&A, 350, 148

Wheelwright, H. E., Weigelt, G., Caratti o Garatti, A., & Garcia Lopez, R. 2013, A&A, 558, 116

White, N. E., Mason, K. O., Huckle, H. E., Charles, P. A., & Sanford, P. W. 1976, ApJ, 209, L119

Willson, L. A. 2000, ARA&A, 38, 573

Wright, A. E., & Barlow, M. J. 1975, MNRAS, 170, 41

Wright, E. L., et al. 2010, AJ, 140, 1868

Zickgraf, F.-J. 1998, in: B[e] stars Paris workshop, Eds Anne Marie Hubert and Carlos Jaschek, Dordrecht; Boston: Kluwer Academic Publishers, ASSL, 233, 1

Zickgraf, F.-J., Wolf, B., Leitherer, C., Appenzeller, I., & Stahl, O. 1986, A&A, 163, 119

This 2-column preprint was prepared with the AAS LaTeX macros v5.2.